Control of laminate quality for parts manufactured using the resin infusion process

Smr M R Kazmi, Quentin Govignon, Simon Bickerton

▶ **To cite this version:**

Smr M R Kazmi, Quentin Govignon, Simon Bickerton. Control of laminate quality for parts manufactured using the resin infusion process. Journal of Composite Materials, 2019, 53 (3), pp.327-343. 10.1177/0021998318783308 . hal-01825552v2

HAL Id: hal-01825552

https://hal.insa-toulouse.fr/hal-01825552v2

Submitted on 20 Jul 2018

HAL is a multi-disciplinary open access archive for the deposit and dissemination of scientific research documents, whether they are published or not. The documents may come from teaching and research institutions in France or abroad, or from public or private research centers.

L'archive ouverte pluridisciplinaire **HAL**, est destinée au dépôt et à la diffusion de documents scientifiques de niveau recherche, publiés ou non, émanant des établissements d'enseignement et de recherche français ou étrangers, des laboratoires publics ou privés.

Control of laminate quality for parts manufactured using the resin infusion process

SMR Kazmi[1], Q Govignon[1,2] and S Bickerton[1]

Abstract

Resin infusion is a manufacturing process used to produce fibre-reinforced thermo-set polymer components. This process is utilised in a range of industries such as aerospace, automotive, marine, rail and defense and is a cheaper method when compared to other closed mould or autoclave manufacturing methods, particularly as the size of the parts increases. In this study, wet compaction characteristics and behaviour of three glass fibre reinforcements were analysed, and 2D panels were manufactured with a selection of inlet and vent pressure combinations during both the filling and post-filling stages of the process to achieve control of the final fibre volume fractions. Reinforcement thickness and resin pressure were monitored throughout each experiment and the achieved fibre volume fractions were measured post-manufacture. Void content was analysed microscopically and related to the respective experimental parameters set. The compaction result fairly predicted the achieved fibre volume fraction of the manufactured part. The possibility of controlling the fibre volume fraction through control of the post-filling pressure was demonstrated. Even though there was a risk of increased void content with some post-filling configurations, the fibre volume fraction could still be controlled without creating voids with careful application of post-filling conditions.

Keywords

Epoxy composite quality, epoxy resin, glass fibres, resin infusion, vacuum-assisted resin transfer moulding

Introduction

When compared to the wet hand lay-up process, resin infusion minimises styrene and other gaseous emission while maintaining simple single-sided mould arrangements.[1] This process also improves part quality, and reduces labour intervention.[2] Industrial resin infusion processing parameters offer very little control over part weight and quality.[3,4] Significant opportunities exist to better control laminate thickness and void content and to improve repeatability of these properties from part to part.[5–9]

Compaction response of a fibre reinforcement layup is a relationship between an applied compression stress on the reinforcement and its thickness or fibre volume fraction. It has been shown to be very influential on the laminate thicknesses during infusion processing, and to final volume fractions achieved in a part. Compaction response can be different for dry and wet fibre reinforcement samples.[10] Careful experiments are required to measure compaction response of fibre reinforcements, in order to forecast the achievable fibre volume fraction (V_f) during manufacturing of composites, or as input for numerical simulation.[11–13] These experiments should follow the compaction path typically experienced by the reinforcement during manufacture. Grimsley et al.,[10] Govignon et al.,[14] Tackitt and Walsh,[15] Grimsley et al.,[16] and Li et al.[17] demonstrated the importance of compaction characterisation in order to predict the maximum achievable fibre volume fraction in a given reinforcement-resin system especially using flexible tooling. Together with the influence of non-elastic reinforcement compaction

[1]Centre for Advanced Composite Materials, Department of Mechanical Engineering, The University of Auckland, New Zealand
[2]Institut Clément Ader (ICA), Université de Toulouse, CNRS, France

Corresponding author:
SMR Kazmi, Centre for Advanced Composite Materials, Department of Mechanical Engineering, University of Auckland, 314 Khyber Pass Road, Auckland 1142, New Zealand.
Email: skaz012@aucklanduni.ac.nz

behaviour, it was found that fibre nesting due to lubrication of the preform by the fluid increases the compressibility of the reinforcing materials at the flow front.[5]

Grimsley et al.,[10] Kuentzer et al.,[18] Tackitt and Walsh,[15] and Williams et al.[2] found out that the resin pressure in the filling stage affects the achieved fibre volume fraction at the end of the resin infusion process and that the compaction behaviour was a combination of resin lubrication and spring-back deformation due to increased resin pressure and decreasing preform pressure. Govignon et al.[5] and Daval and Bickerton[19] stated that two key parameters proven to control laminate quality were the position of vents and combination between the applied injection and post-filling pressures. The position of the vents and the post-filling conditions; both affect the removal of excess resin to equilibrate the distribution of resin pressure and laminate thickness. Moreover, the final compaction state of the laminate depends on both the filling and post-filling conditions and can be affected by the pressure difference between the inlet and vent during filling.[20] Li et al.[16] found that thickness gradient is an outcome of the infusion pressure gradient (driving force of the resin) during the process. Depending on the post-filling conditions, the pressure gradient will evolve during post-filling and might even be completely eliminated. Therefore, the focus of this study is the analysis of different filling and post-filling pressures while keeping the vent positions constant.

The quality of fibre composites is significantly influenced by the procedure constraints and materials used during manufacturing.[19] One of the more significant quality features is the void content in the manufactured part, as this has been shown to have a significant influence on the mechanical properties of the laminate. This is due to the unfavourable effect, which voids have on surface finish and mechanical properties.[7] When resin is unable to fill the vacant spaces between the fibres, air is entrapped and voids are generated.[1] One of the reasons for void generation can be explained through the dual-scale flow between and inside fibre bundles. If the flow is much faster around fibre bundles than within, there will be micro voids trapped inside the bundles. When the macro-scale flow is too slow, the capillary effect will result in resin travelling faster inside the fibre bundles and can result in macro voids between fibre bundles.[18,21–25] Another reason for void formation is resin boiling off or releasing volatile compounds during the filling or the post-filling stage. The size of porosities is also affected by the resin pressure inside the laminate, since a constant mass of trapped gas will expand in volume as the pressure surrounding it decreases. Kuentzer et al.[18] realised that the addition of resistance at the vent and resin bleeding reduced the void content. Resin bleeding in case of vacuum-assisted resin transfer moulding (VARTM) is the practice of continuing the injection of resin for some time once the whole mould is filled as opposed to clamping the inlet to stop resin injection. The so-called ''brake'' region resists flow and creates a significant pressure difference between the vent and the end of the reinforcement near the vent.[14] A brake permits a complete saturation of the reinforcement before the resin front reaches the vent, and minimises the amount of resin wastage through the vent. By reducing pressure and thickness gradient along the part it also helped homogenise the final laminate properties.

Figure 1 schematically demonstrates the basic steps in a resin infusion process. In this research, these steps were followed as a guideline and were modified to suit the requirements of the experiment. The process consists of four stages: lay-up, pre-filling, filling and post-filling. During pre-filling vacuum is applied, and as the

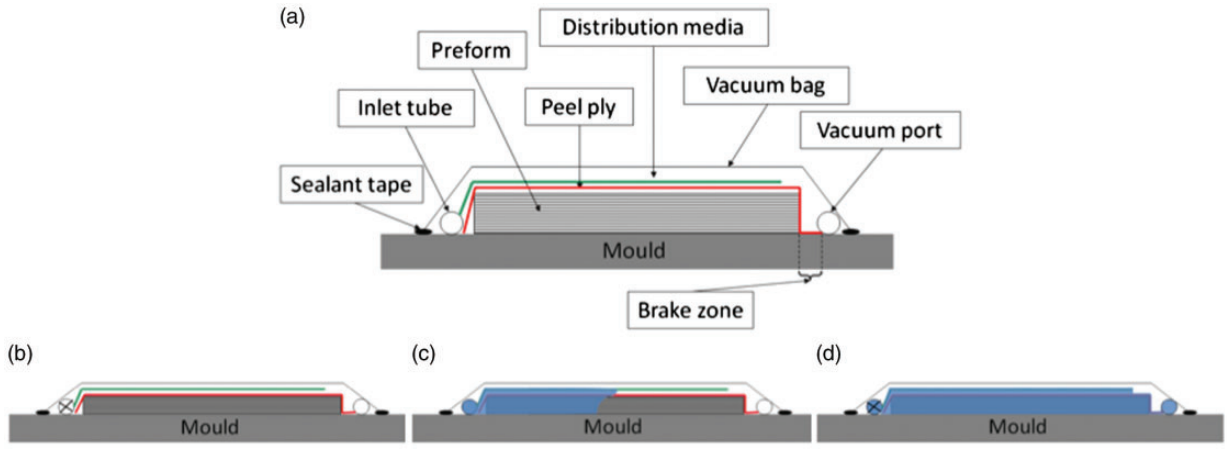

Figure 1. Schematic diagram of the steps in resin infusion. (a) Lay up. (b) Pre-filling. (c) Filling. (d) Post-filling.

pressure differential between the cavity and the atmospheric pressures increases, the dry reinforcement is compacted. Debulking is the process of cycling compaction/unloading of the fabric during pre-filling to reduce thickness and hence achieve a higher fibre volume fraction (V_F);[26] this was also found to reduce the compressive variability of the dry reinforcement.[27,28] For standard resin infusion, it is common procedure for at least one debulking cycle to occur during pre-filling when the operator checks the leak proof environment created by vacuum bagging around the mould. During the filling stage, vacuum is maintained in the cavity while the inlet is opened with resin arriving at atmospheric pressure. The applied vacuum not only compresses the reinforcement but also provides the pressure gradient that drives the resin into the mould cavity. The post-filling stage starts once all of the reinforcement has been saturated. Different post-filling strategies can be implemented by either applying a desired level of vacuum or clamping at both the vent and the inlet. The post-filling conditions are maintained while the resin gels and then cures.

Materials

Fibre reinforcements

Three glass fibre reinforcement styles were utilised in this study. All three reinforcements were non-crimp, stitched reinforcements with a similar areal weight but with different architecture. Figure 2 shows close-up images of each reinforcement, illustrating the size and spacing of fibre bundles within each of the three characterised reinforcements named as EQ-850, EB-825 and EDB-800, and supplied by GURIT. EQ-850 is a quadri-axial non-crimped reinforcement with an areal density of 850 gsm. There are four layers of fibre bundles stitched together, which are at angles of 0, 90°, +45°, and –45° relative to the roll direction. EB-825 is a biaxial non-crimped reinforcement having two layers of fibre bundles, which are at angles of 0 and 90° to the roll direction, it has an areal density of 825 gsm. EDB-800 is a double biaxial non-crimped reinforcement with an areal density of 800 gsm. Only two layers of fibres at angles of +45° and –45° make up this reinforcement. Qualitatively, from Figure 2 it can be observed that EB-825 has the widest fibre bundles and gaps between bundles, while EDB-800 has the smallest fibre bundle width.

Fibre reinforcement compaction characterisation

In order to predict the variability and the achievable fibre volume fraction range, the compaction behaviour of the three reinforcements was characterised.

In order for the characterisation to be representative of the infusion process, the layup of the compaction sample was similar to that used for infusion experiments. For all the fibre reinforcement styles, eight fabric layers were stacked to make the preform for both the compaction and resin infusion experiments. The orientation of all the fabric layers for EQ-850 and EDB-800 were along the roll direction. For the EB-825 fabric, four layers were along and four were perpendicular to the roll direction. The fabric layers were alternated in such a way that if the first layer was along the roll direction, the second one was perpendicular to the roll direction and the same pattern continued for the rest of the layers. All the compaction tests were performed using an Instron 1186 universal testing machine. The reinforcement samples were cut in a circular shape (265 mm diameter). The reinforcements were subjected to a cycle of dry compactions and relaxation (to reproduce the loading history applied during the pre-filling stage with leak checking), before a cycle of wet relaxation and compaction (reproducing the filling and post-filling stages), as schematised in Figure 3. The fibre volume fraction was calculated from the

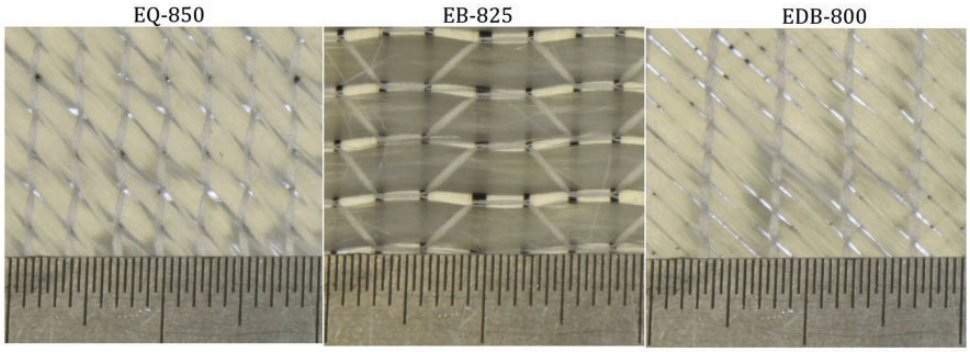

Figure 2. Close-up images of the EQ-850, EB-825, and EDB-800 reinforcements. A ruler having 0.5 mm steps is included to demonstrate the material scale.

measured thickness values and plotted against compaction stress. The results were then used to determine the range of applied resin vacuum pressure in the post-filling stage. To simulate the presence of a viscous resin during the filling and post-filling stages of resin infusion, a mineral oil, supplied by Kauriland Petroleum (product name Mobil DTE Light), was injected into the compaction sample 5 min after the end of the dry compaction cycle (Figure 3).[14] The oil was injected through a 5 mm hole in the centre of the lower platen of the compaction jig. The filling time for both EQ-850 and EDB-800 samples was around 2 min and 1 min for the EB-825 sample. Compaction tests were repeated four times to investigate variability in compaction response due to variation in structure within a layer and nesting between the layers.

Figure 4 presents the averaged results from the wet compaction of the three fibre reinforcements, and serves to compare between the ranges of achievable V_F for the three reinforcements. The results show that EQ-850 and EDB-800 reinforcements have the potential to achieve a higher fibre volume fraction as compared to EB-825.

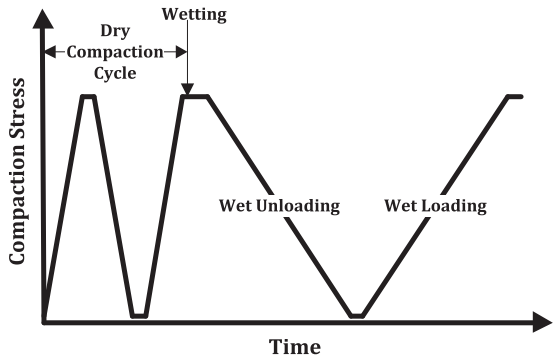

Figure 3. Schematic of compaction cycle for material characterisation.

Resin selection

It was important to complete this experimental study with a resin system commonly used in industry. This was necessary to have an idea about the effects of the curing of resin, vacuum compaction and post-filling conditions on the resin and final laminate quality. PRIME^{TM} 20 epoxy infusion system supplied by GURIT, was utilised in all resin infusion experiments. The resin-hardener combination used allowed a resin gel time of approximately 90 min at standard temperature and pressure.

Resin infusion experimental programme

Experimental setup

Figure 5 presents a schematic diagram of the resin infusion experimental setup used in this research. The viscosity and cure kinetics of epoxy resins are dependent on their temperature.[29,30] It was therefore decided to improve consistency by performing all experiments at 25°C. An enclosure was designed and assembled to create a temperature controlled chamber around the mould. To allow the use of stereophotogrammetry[31,32] for full field measurements of laminate thickness, the top of the enclosure was made of glass, ensuring good transparency and minimal image distortion.

A vacuum system was required to implement a standard resin infusion process, and to allow for pressure control at the resin inlet and vent. The pump and catch-pots have been arranged as shown in Figure 5, to

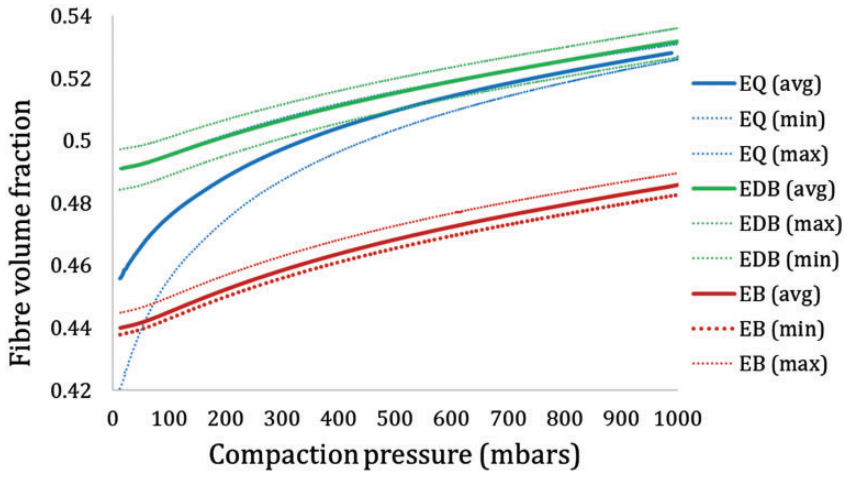

Figure 4. Average wet loading curves for the three reinforcements.

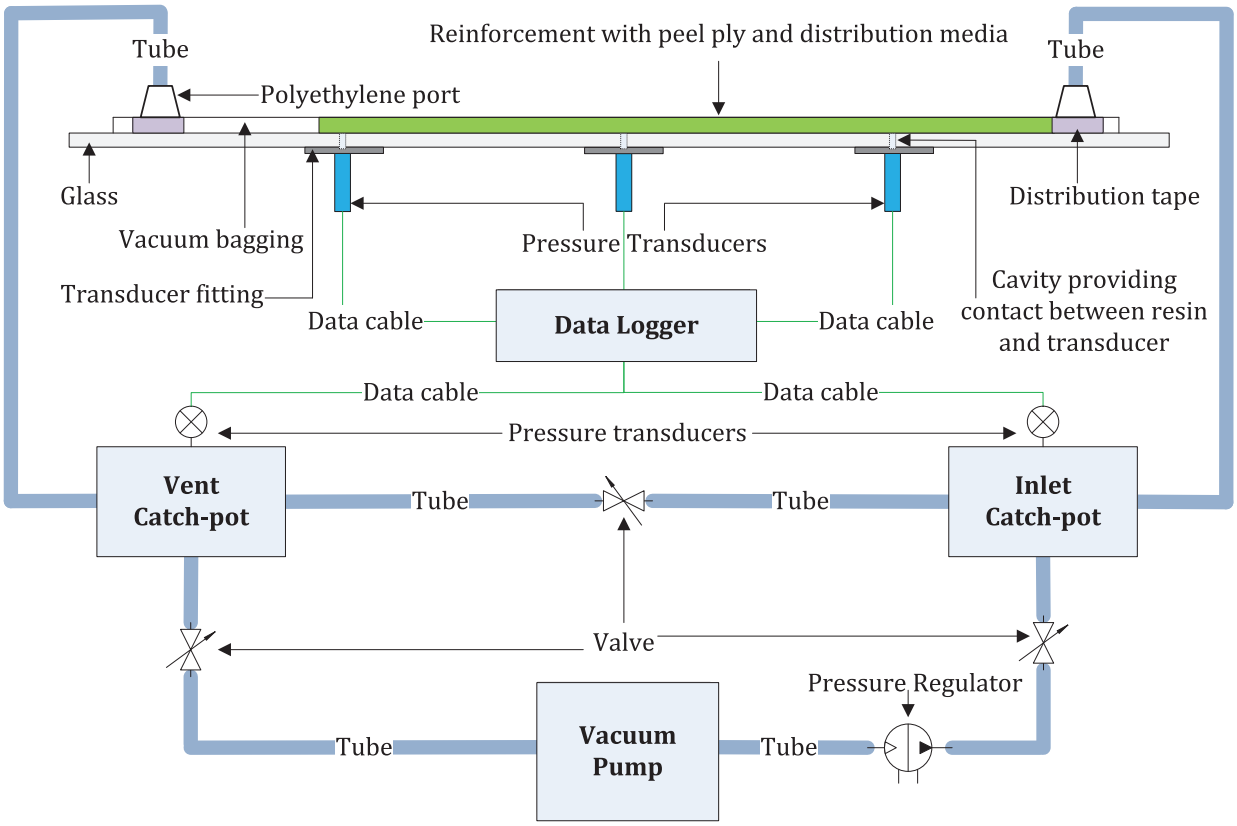

Figure 5. Schematic of the resin infusion setup.

achieve this. Pressure transducers (Edwards ASG 1000 mbar, supplied by VABS) were used to monitor pressures in the inlet and the vent catch-pots during the experiment. These transducers were also used during the leak checks of the mould. Three pressure transducers (*BTE6001A4-FL* from *Farnell*) were used to monitor resin pressure inside the laminate along the mould surface at the location of the drilled holes. Aluminium fittings were used to attach the pressure transducers to the glass mould, forming a sealed cavity between the glass and the transducer. Silicone gel was used as a cover on the transducers to protect the transducer diaphragm from the thermoset resin.

Experimental procedures

Figure 6 presents the dimensions of the materials used and their positions on the glass mould. The region between the reinforcement and the vent distribution tape was kept constant because it is thought to govern the evolution of pressure within the laminate once the resin flow front enters this region. Distribution tapes, distribution media, peel ply, polyethylene vacuum tubes, reusable polyethylene ports as inlet and vent and a PA6 (Nylon) 50 μm thick vacuum bag were used following the standard resin infusion process. The captions 'Pos1' to 'Pos6' as used are positions on the laminate. The three transducers employed in the experiments, were situated at positions 2, 4 and 6. 'I' and 'V' symbols represent the inlet and vent.

In this research, during the pre-filling stage, the preform was subjected to a cycle of full vacuum (995 mbar compaction pressure) applied for 10 min, then left under no vacuum for the next 5 min and then again put under full vacuum for 5 min just before the filling stage. During this time before the filling stage could be started, resin was mixed with the hardener, initial thickness of the reinforcement was measured with a dial gauge, a leak check was performed and the resin mixture was degassed. The dial gauge used was a Mitutoyo digital dial indicator with an accuracy of 0.01 mm. It was first set to zero on contact with the mould before lay-up.

In the post-filling stage, the vent was set to the required post-filling pressure, and the inlet and vent catch-pots were then connected. This was the case for all experiments except those in which the inlet was clamped in the post-filling stage.

All stages were performed under a temperature of 25°C maintained inside the enclosure; the finished laminate was left, in the post-filling condition, for 12 h inside the enclosure. After demoulding, a post-

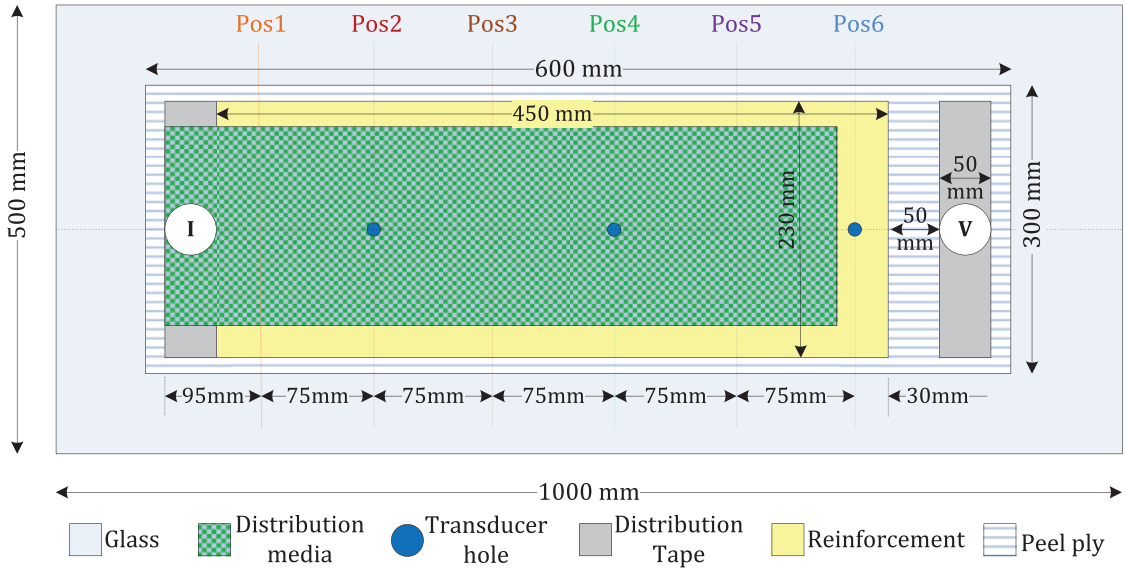

Figure 6. Schematic for material placement and data processing points.

cure thermal cycle was applied following the Prime 20 specification sheet.[33] The post cure cycle involved maintaining the laminate at 65°C for 7 h.

Experimental plan

In industry it is common practice to clamp the inlet at the onset of post-filling. In the industrial process with a break region and clamped inlet, the internal laminate pressures come down very slowly and the final fluid pressure depends mainly on the ease of resin flow through the brake zone between the vent and the reinforcement, which is often not well controlled. Due to the large size of the manufactured parts, a thickness gradient often prevails along the laminate length resulting from the pressure gradient, especially when the mould inlet and vent are more than a metre apart. This can be minimised if the pressure values at the inlet and vent are set to be equal. In addition to this, pulling vacuum through the inlet also enables faster removal of the excess resin situated at the inlet, since it then does not have to travel through the full length of the part. In this study, the industrial method was compared to this latter technique. The post-filling stage was initiated by changing the inlet to a vent, to achieve a specific residual pressure in the laminate and hence a particular fibre volume fraction. The inlet was converted to the vent when all the reinforcement was saturated with resin, to make sure that enough resin surrounded the reinforcement, and that on application of a particular post-filling pressure, the surrounding resin could fill the reinforcement if required.

Table 1 presents the filling and post-filling conditions used for the resin infusion trials. The post-filling pressures for these trials were kept at 0, 500 and 900 mbar to maximise the range of V_F that could be achieved. For EQ-850 only, the filling procedure was changed by putting the inlet at 650 mbar (350 mbar compaction pressure). This was selected to check the effect of slower filling on the final quality of the laminate in terms of the void content. The letter 'r' in the experimental codes implies a repeat experiment. If 'r1' is the first repeat experiment, 'r2' is the second repeat experiment.

To validate the consistency and repeatability of the experimental procedure, while minimising the time and material consumption of these experiments, only some selected experiments were repeated. These were the ones with 5 and 900 mbar post-filling pressures for EQ-850 and only the 5 mbar post-filling pressure for EB-825 and EDB-800 due to time constraints.

Results and discussion

Effect of clamping vs. turning inlet into a vent

Figure 7 shows the resin pressure evolution for an experiment utilising EQ-850, in which the inlet is clamped in the post-filling stage. It also shows that resin pressure at the pressure transducer locations did come down slowly until gelation of the resin at about 85 min, and remained above 400 mbar. The resin pressure in the experiment where the inlet was clamped, took longer to stabilise than in cases where the inlet was turned into a vent. This is due to the resistance to flow created by the brake region between the reinforcement and the vent. The brake region takes up most of the pressure gradient between inlet and

vent, and restricts greatly the flow of resin through it, thus limiting the resin pressure decay in the laminate.

Figure 8(a) to (c) shows the resin pressure and laminate thickness evolution for EQ-A/0 experiment at the post-filling pressures of 5, 500 and 900 mbar. Since the resin pressure in the EQ-A/0 experiment reduced down very close to 5 mbar almost 10 min after applying the post-filling conditions, the thickness achieved in the final part was lower than that in the clamped experiment (Figure 7). This is because the vacuum applied from the inlet, allows the excess resin to flow out of the reinforcement without going through the brake region. Furthermore, since most of the excess resin is situated close to the inlet, it is not required to flow through the length of the laminate, taking the shortest path out of the inlet. When larger pressures were applied at the inlet (see Figure 8(b) and (c)), both resin pressures within the laminate and laminate thickness equalised to larger values. This was as expected, demonstrating the potential for controlling final part fibre volume fraction. In Figures 7 and 8, the inlet pressure was less than 1000 mbar. The inlet pressure did not quite reach 1000 mbar as it represents the pressure in the catch-pot under atmospheric pressure and not the absolutely ambient atmospheric pressure.

Table 1. Infusion schedule.

		Filling pressures (mbar)		Post-filling pressures (mbar)	
No.	Code	Inlet	Vent	Inlet	Vent
1	EQ-A/0	1000	5	5	5
2	EQ-A/C	1000	5	Clamped	5
3	EQ-A/500	1000	5	500	500
4	EQ-A/900	1000	5	900	900
5	EQ-650/500	650	5	500	500
6	EQ-650/900	650	5	900	900
7	EQ-650/0	650	5	5	5
8	EQ-A/0_r1	1000	5	5	5
9	EQ-A/900_r1	1000	5	900	900
10	EQ-A/500_r1	1000	5	500	500
11	EQ-A/C_r1	1000	5	Clamped	5
12	EQ-A/0_r2	1000	5	5	5
13	EQ-A/900_r2	1000	5	900	900
14	EB-A/0	1000	5	5	5
15	EB-A/900	1000	5	900	900
16	EB-A/500	1000	5	500	500
17	EB-A/C	1000	5	Clamped	5
18	EB-A/0_r1	1000	5	5	5
19	EDB-A/0	1000	5	5	5
20	EDB-A/900	1000	5	900	900
21	EDB-A/500	1000	5	500	500
22	EDB-A/C	1000	5	Clamped	5
23	EDB-A/0_r1	1000	5	5	5

Effect of filling pressures

Three experiments were completed in which the filling pressure gradient was reduced by dropping the inlet (resin pot) pressure from atmospheric pressure to 650 mbar, while maintaining the vent at full vacuum. The post-filling pressures were set to 0, 500 and 900 mbar. Figure 9 presents results from one of the experiments with a 900 mbar post-filling pressure.

Comparing only the filling stage of the two experiments in Figures 9 and 8(c), it can be seen that a lower pressure gradient was present during the filling stage of the 650/900 experiment. This resulted in a reduced

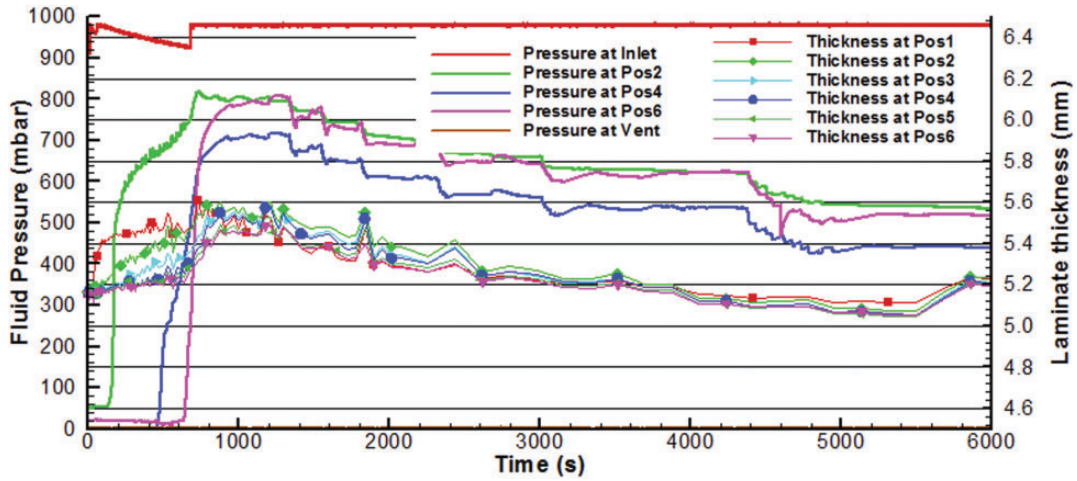

Figure 7. Resin pressure and thickness progression during EQ-850 experiments with atmospheric filling and clamped inlet during post-filling.

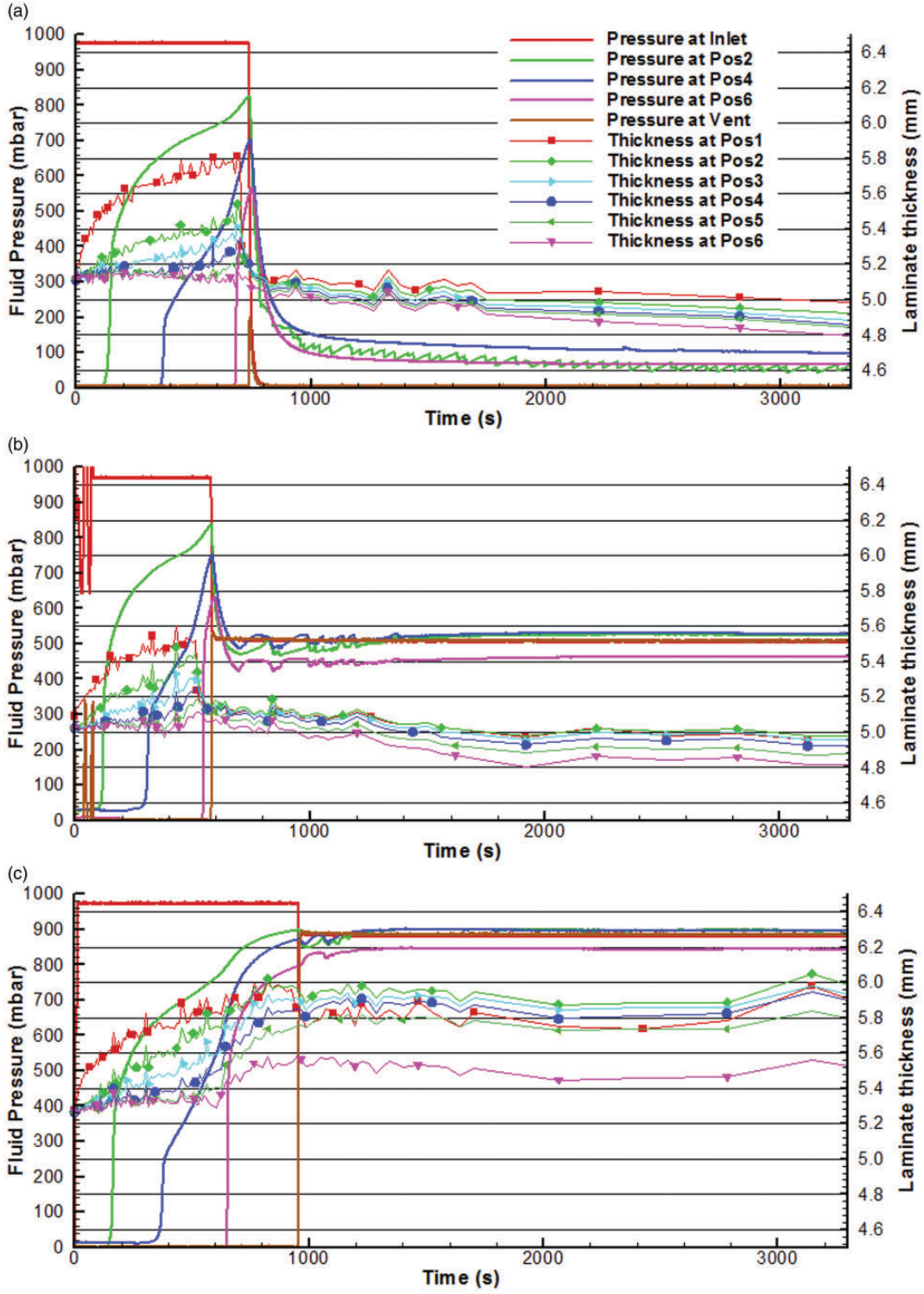

Figure 8. Resin pressure and thickness progression during EQ-850 experiments with atmospheric filling and (a) 5 mbar, (b) 500 mbar and (c) 900 mbar post-filling pressure.

thickness gradient induced, and hence the thickness values are much closer to each other in Figure 9 as compared to Figure 8(c). In addition, the fill time for both these experiments was significantly different because of the difference in the pressure gradient. For the A/900 experiment the fill time was around 10 min but for the 650/900 experiment it is around 26 min. Although the thickness gradient along the laminate

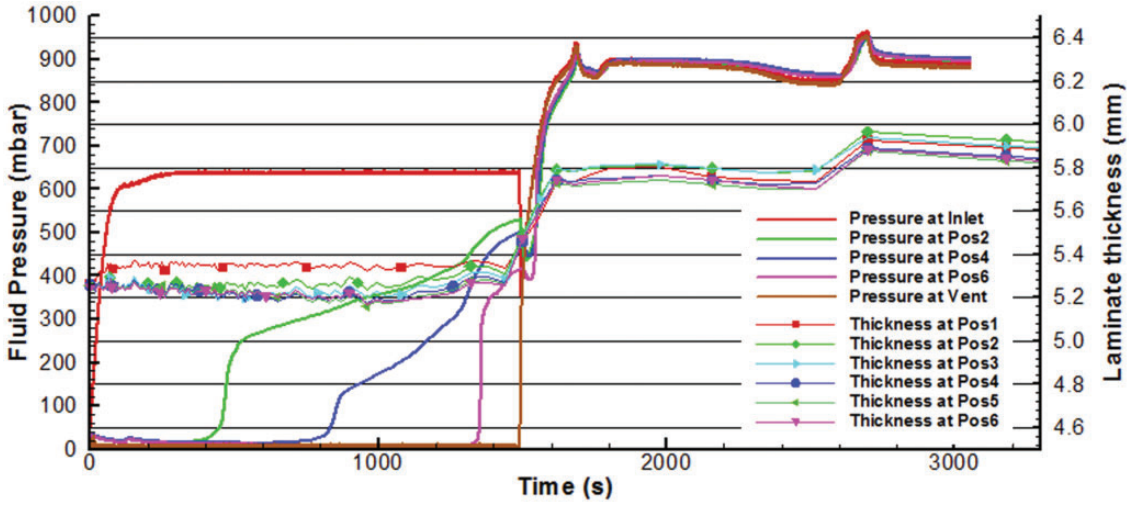

Figure 9. Resin pressure and thickness progression during EQ-850 experiments with 650 mbar filling inlet pressure and 900 mbar pressure during post-filling.

was decreased, the total manufacturing time almost tripled.

Effect of post-filling pressures

Using Figure 8, a relationship between the post-filling pressure and the final laminate thickness can be deduced. For the A/0 experiment, the thickness at position 1 decreased from 5.8 mm at the time of the application of the post-filling pressure to 5.0 mm at the end of the experiment. For the A/500 experiment it decreased from 5.4 mm to 5.0 mm and for the A/900 experiment, it increased from 5.4 mm to 5.8 mm. The A/0 experiment produced high fibre volume fraction laminate, while the A/900 experiment produced a low fibre volume fraction laminate. It can therefore be inferred that regulation of the post-filling pressure at the inlet allows some control of the thickness, and hence the fibre volume fraction of the laminate.

Accuracy of data acquisition

In Figures 7 to 9, the pressure and thickness curves are oscillating. The oscillations in the pressure curves were mostly at the onset of post-filling in Figures 7 and 8. The oscillations of the pressure during post filling appear to be linked to the very slow flow occurring when the inlet is clamped (Figure 7) or when the pressure has almost equilibrated (Figure 8). For the experiment presented in Figure 9 the pressure regulator had some uncontrolled issues to maintain the pressure at 900 mbar, which led to instability in the pressure and hence the thickness measurements.

The oscillation in the thickness data can be due to noise in the digital image correlation technique and ambient vibration causing vibration of the rig. It was made sure that the experiments are done late in the evening when most of the students or researchers in the lab have finished their work. Still there were machines in the lab that had to run overnight and because of the sound and vibration of those machines, oscillations can be seen clearly in the thickness curves.

The frequency of the DAQ is 1 Hz for the pressure and the image acquisition used for the thickness measurement was set at one image every 2 s during the filling and one image every 5 s during post-filling.

Final part analysis

The void content in the final part was investigated both quantitatively and qualitatively, and the fibre volume fractions calculated in a number of ways to account for experimental errors. Void content was also analysed using microscopy image analysis.

Achieved fibre volume fractions

Fibre volume fraction of the manufactured laminates was calculated from different sources and compared to the fibre volume fraction predicted from the compaction data. Furthermore, mass fraction of the manufactured laminates was used to estimate the theoretical fibre volume fraction. This was compared with the experimental fibre volume fraction to give a qualitative indication of the void content in the manufactured laminates.

Thickness at 12 points on the manufactured laminate were measured after each experiment; three readings being taken across the width of the part along positions 1, 2, 4 and 6 (see Figure 6). The thickness was measured at Positions 2, 4 and 6 as they correspond to the

positions of the pressure transducers and could therefore be directly correlated to the locally applied pressure. Thickness at Position 1 was also measured because it was closest to the inlet while being far enough to ensure that there was no edge effect. These thickness values were averaged and the average thickness of the laminate was used to calculate its fibre volume fraction termed as V_{FP} in the following equation

$$V_{FP} = \frac{M_A.n}{\rho_F.h} \tag{1}$$

where M_A is the areal density of the respective reinforcement's fabric layer, ρ_F is the density of the dry reinforcing fibre (i.e. 2580 kg/m^3), n is the number of fabric layers, and h is the average laminate thickness determined by using the physically measured thickness of the manufactured laminate at 12 points (3 points each at positions 1, 2, 4 and 6). There will be ±5% percentage uncertainty in M_A, which is a common value of variation of the superficial density of the reinforcement due to variability in the manufacturing process.

V_{FM} is the fibre volume fraction calculated based on the fibre weight fraction, using the measured masses of dry reinforcement and the manufactured laminate in equation (2), the mass of resin was calculated to be the difference between the mass of dry reinforcement and that of the manufactured laminate. In this calculation, it was assumed that the voids in all the laminates were either equal or zero

$$V_{FM} = \left(\frac{m_F}{\rho_F}\right) \div \left(\frac{m_F}{\rho_F} + \frac{m_L - m_F}{\rho_M}\right) \tag{2}$$

where m_F is the measured mass of dry reinforcement, ρ_F is the density of the dry reinforcing fibre (i.e. 2580 kg/m^3), m_L is the measured mass of the manufactured laminate and ρ_M is the density of the resin matrix. Equation (2) can also be written as follows

$$V_{FM} = Vol_{DR} \div (Vol_{DR} + Vol_R) \tag{3}$$

where Vol_{DR} is the volume of dry reinforcement and Vol_R is the volume of the resin. The density of the cured resin was found by using the rule of mixture from the values in the PRIME^{TM} 20LV specification sheet. The calculated value of ρ_M was 1.1449 g/cm^3.[33]

V_{FM} values were compared with the V_{FP} values and the difference was divided by V_{FM} values to obtain a percentage difference. This difference gives a rough idea of the void content in the manufactured laminates and was calculated using the following equation

$$P_E = \left(\frac{V_{FM} - V_{FP}}{V_{FM}}\right) \times 100 \tag{4}$$

Terzaghi's relation ($\boldsymbol{\sigma_C} = \mathbf{P_A} - \mathbf{P_R}$) relates the applied compaction stress on the reinforcement $\boldsymbol{\sigma_C}$ to the atmospheric pressure $\mathbf{P_A}$ and the fluid pressure $\mathbf{P_R}$. $\mathbf{P_R}$ is also the pressure within the cavity. The laminate fibre volume fraction predicted by the wet compaction of the reinforcements was termed as V_{FC}. V_{FC} is the fibre volume fraction predicted from the compaction data at the corresponding compaction pressure. V_{FC} is calculated employing equation (2) and using the thickness measurement of the fibre reinforcement wetted with oil shown in the compaction data (Figure 4). It was assumed that the oil used to impregnate the fibre reinforcement in the compaction experiments, replicate the lubricating effect from the epoxy resin used to manufacture the laminates. For example, if the final average laminate pressure is 20 mbar, a fibre volume fraction corresponding to 980 mbar of compaction pressure was read from the curves provided in Figure 4.

Table 2 presents V_{FP}, V_{FC}, V_{FM} and the percentage difference values for all the manufactured laminates and their corresponding final average pressures achieved at the end of the post-filling stage. The post-fill time is the time taken after the onset of post-filling until the resin pressure fluctuation reduced to ± 5 mbar/min.

Looking at the percentage difference data presented in Table 2, it is observed that as the vacuum applied during post-filling is increased, a greater content of voids was present in the laminate. There are few outliers, which can be expected due to the approximations in the values of V_{FP} and V_{FM} and experimental errors.

Figure 10 shows a graphical representation of V_{FP} values and V_{FC} curves. The curves represent the variation of the volume fraction of the respected wet fibre reinforcement under compaction from 0 to 1000 mbar (Figure 4). The points in these plots represent the fibre volume fraction values calculated using the average of the three thickness values obtained experimentally at the inlet, Position 2 (Pos2), Position 4 (Pos4) and Position 6 (Pos6) as shown in Figure 6. The curves in Figure 10 were extracted from the compaction data (Figure 4). The V_{FP} measured after the infusions were plotted in Figure 10 at the compaction level of three applied post-filling pressures: 100 mbar (implies 900 mbar of post-filling pressure), 500 mbar (implies 500 mbar of post-filling pressure) and 1000 mbar (implies 0 mbar or full vacuum post-filling pressure).

Figure 10 allows one to compare the predicted fibre volume fraction from the material compaction characterisation, and the achieved fibre volume fractions of the manufactured laminates using resin infusion. It can be concluded that for all three reinforcements, compaction characterisation provides a good estimation of the behaviour and of the range of achievable fibre volume fraction via resin infusion. For EQ-850 and EDB-800,

Table 2. Comparison of fibre volume fractions.

No.	Code	Fill time (s)	Post fill time (s)	Final average laminate pressure (mbar)	Fibre volume fraction (compaction), V_{FC}	Fibre volume fraction (physical), V_{FP}	Fibre volume fraction (mass), V_{FM}	Percentage difference (V_{FP} and V_{FM}) (%)
Panel a: EQ infusion trials								
1	EQ-A/0	480	500	100	0.53	0.52	0.55	6.2
2	EQ-A/0_r1	625	1000	20	0.53	0.52	0.55	5.8
3	EQ-A/0_r2	750	1500	60	0.53	0.52	0.57	11
4	EQ-650/0	2150	800	390	0.52	0.51	0.54	5.8
5	EQ-A/500	750	2200	480	0.52	0.51	0.53	4.5
6	EQ-A/500_r1	600	1500	490	0.52	0.51	0.52	4.2
7	EQ-650/500	1570	1000	480	0.52	0.51	0.53	3.0
8	EQ-A/C	870	3000	710	0.52	0.51	0.52	3.5
9	EQ-A/C_r1	750	5000	490	0.51	0.49	0.53	4.1
10	EQ-A/900	510	400	880	0.49	0.47	0.48	1.5
11	EQ-A/900_r1	480	600	910	0.49	0.47	0.50	5.3
12	EQ-A/900_r2	900	1000	870	0.49	0.47	0.50	5.8
13	EQ-650/900	1500	600	850	0.49	0.47	0.50	6.6
Panel b: EB infusion trials								
14	EB-A/0	320	1200	80	0.47	0.47	0.55	17
15	EB-A/0_r1	310	2000	60	0.47	0.47	0.56	17
16	EB-A/500	310	400	490	0.47	0.47	0.50	6.6
17	EB-A/C	320	3500	530	0.47	0.45	0.47	5.1
18	EB-A/900	300	600	790	0.45	0.43	0.46	8.0
Panel c: EDB infusion trials								
19	EDB-A/0	460	700	80	0.53	0.54	0.58	6.4
20	EDB-A/0_r1	830	1000	30	0.53	0.56	0.58	2.6
21	EDB-A/500	550	700	500	0.52	0.51	0.52	1.7
22	EDB-A/C	470	3500	440	0.52	0.53	0.54	2.2
23	EDB-A/900	440	400	900	0.49	0.52	0.52	0.1

the achieved fibre volume fraction (V_{FP}) matches the fibre volume fraction (V_{FC}) predicted using the compaction results quite well. For EB-825, the trend of the V_{FP} values and the V_{FC} curve is matching but there is a clear off-set of –0.02. Further experiments will be required to prove whether this offset is constant. If it is, then the compaction results can be calibrated to predict the fibre volume fraction of the EB-825 and EDB-800 laminates.

According to Summerscales, using reinforcements in which the fibre bundles are tightly packed and closely spaced within the reinforcement, laminates with high fibre volume fraction and low void content can be expected.[1] EDB-800 is an example of such a fibre reinforcement, because it produced laminates with a higher fibre volume fraction and lower void content. On the contrary, EB-825 had a lower resistance to resin flow, making resin filling and removal quicker than for the other reinforcements. EB-825 laminates had the lowest filling times, the lowest fibre volume fraction and the highest void content values (Table 2 (panels b and c)).

Void content microscopic analysis

Two 25 mm square samples each were cut from the manufactured laminates at three positions (inlet, mid and vent), so that the laminate cross sections could be observed under an optical microscope. Figure 11 presents micrographs of samples from the 650/0 and 650/500 EQ laminates. Voids can be seen both near the inlet and vent samples from the EQ-650/0 experiment, unlike the mid sample that is almost void free. This implies that the voids are due to the sudden change of a pressure of 650 mbar as soon as the post-filling pressure is applied. Since the middle part of the laminate is further away from the inlet or vent, this sudden change does not induce voids there. For the 650/500 experiment, samples from the mid and vent positions are almost

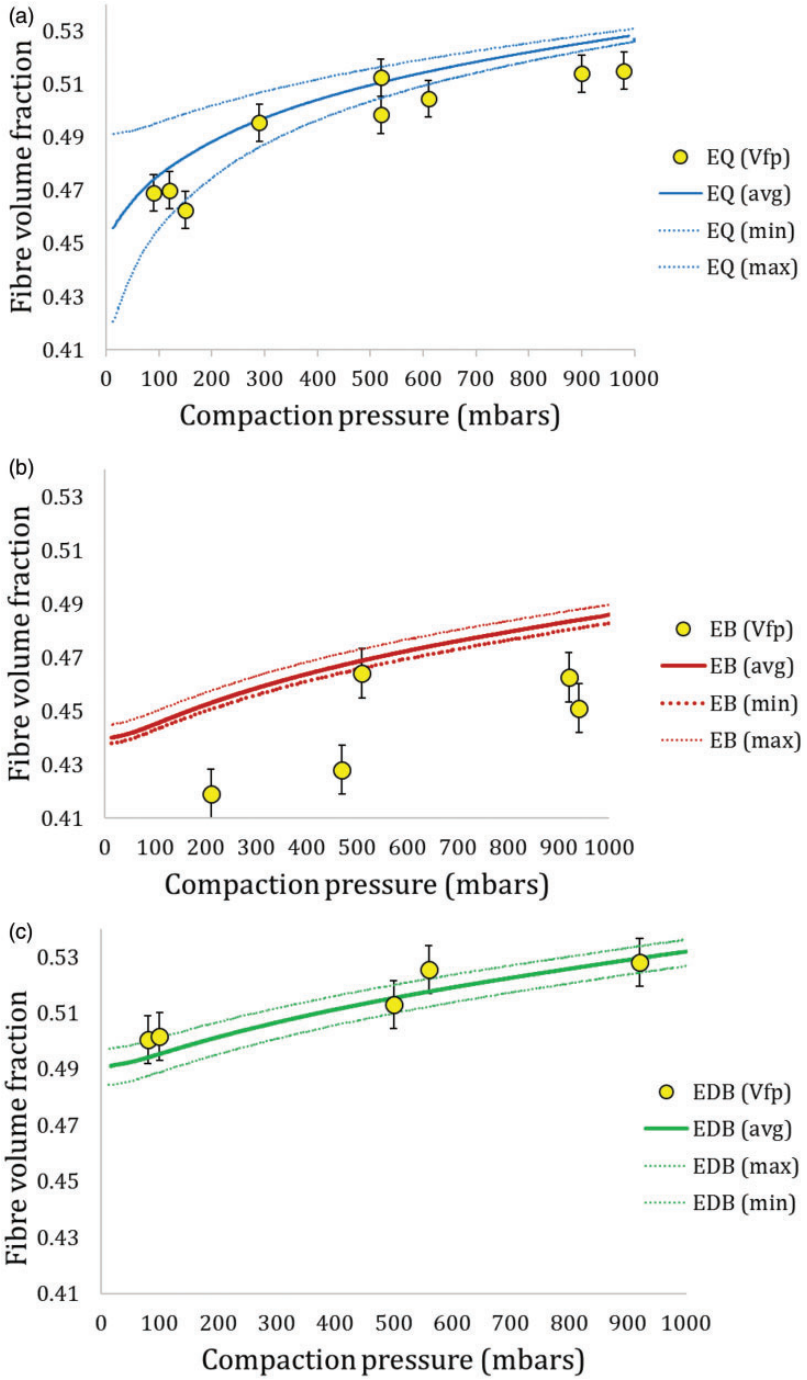

Figure 10. VFC plots and VFP values for: (a) EQ-850, (b) EB-825, and (c) EDB-800.

void free, and the inlet position has very few voids. This is because when vacuum was pulled in the post-filling stage for both experiments, the 650/500 experiment's inlet had to drop only 150 mbar as compared to a drop of 650 mbar in the 650/0 experiment.

Figure 12 presents micrographs of samples from the A/0, A/500 and A/900 EDB laminates. EDB samples were dominated by micro voids due to this material's compact fibre architecture. For the EDB A/0 experiment, at the onset of the post-filling stage, there is an approximate a 900 mbar compaction increase at the inlet, but almost no compaction change at the vent. So in this case, the vent must have fewer voids than the inlet. As can be seen in Figure 12, the voids at the A/0 vent are fewer than those at the inlet, but even the voids at the inlet are negligible. This is because when vacuum is applied at the inlet, the volume of the laminate decreases, and the excess resin at the inlet leaves

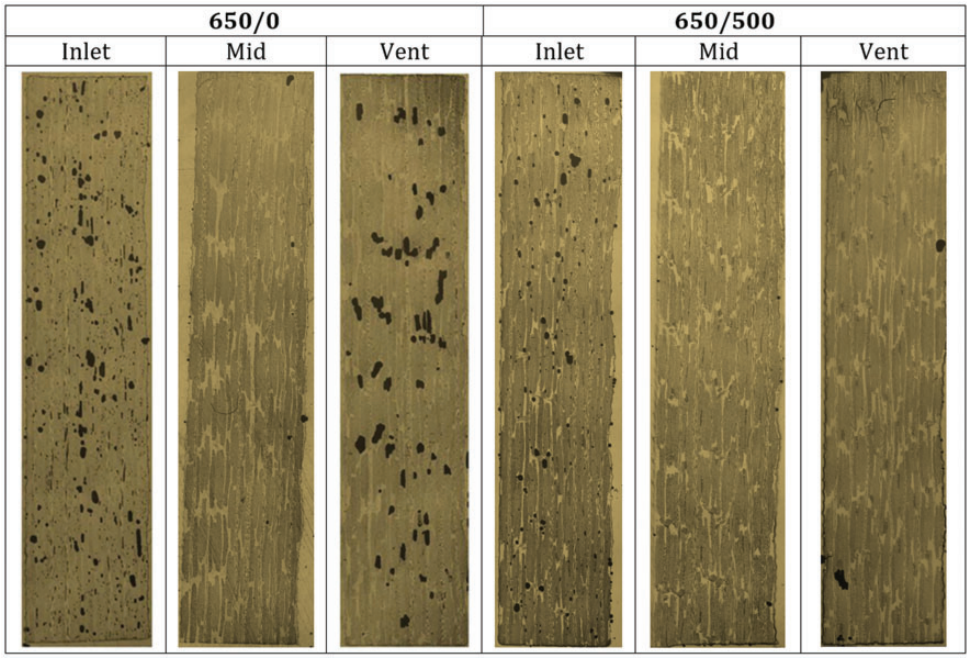

Figure 11. Cross-sectional microscopic images of EQ-850 experiments near the inlet, mid and vent.

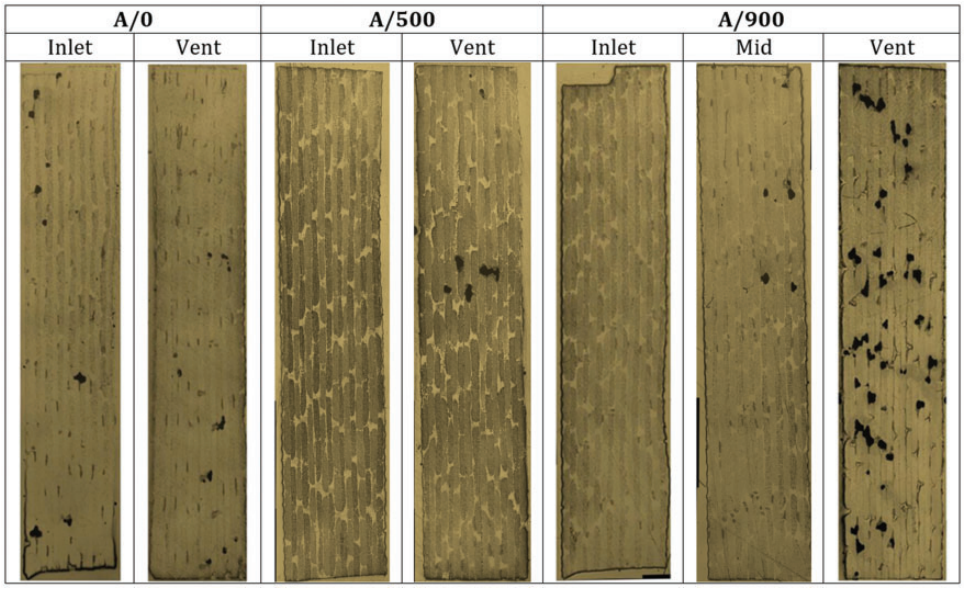

Figure 12. Cross-sectional microscopic images of EDB-800 near inlet, mid and vent.

the laminate. However, since there is already more than enough resin at the inlet, this change does not induce many voids at the inlet. The inlet and the vent samples for the A/500 experiments have a similar quantity of voids because of a similar pressure change at both points at the onset of the post-filling stage. The A/900 experiment produced voids only at the vent, while the inlet and mid samples were almost void free. This is due to the fact that at the onset of the post-filling stage there is a 900 mbar compaction decrease in the A/900 laminate near the vent, but an approximate 100 mbar compaction increase at the inlet. At the vent, because of this sudden change, the reinforcement increases in volume and hence extracts all the surrounding resin available. It can be assumed that there was not enough surrounding resin to fill the increasing volume, particularly near the vent, and that voids were generated due to the suction of air near the vent. The EDB laminates generated

the lowest void contents compared to the other two reinforcements. There is not much difference in void content if we compare the EDB-A/0 and EDB-A/900 laminates. The EDB reinforcement has a lower permeability due to its fibre architecture so it is more restrictive to resin flow. Therefore, during the post-filling stage, very few voids were generated due to the quick resin removal at the inlet or vent in the A/0 experiment, but more voids were generated when a quick resin filling was required at the vent position of the A/900 experiment.

Figure 13 presents micrographs from samples of the A/0, A/C and A/900 EB laminates at the inlet, mid and vent positions. EB laminates generated more voids than any other reinforcement. This was particularly true for the A/0 experiment because of the less dense packing of fibre bundles in the EB reinforcement. The middle of all laminates had very few voids, indicating that most voids were created during the post-filling stage. The voids created during the post-filling stage were due to the excess resin removal from the reinforcement in case of A/0 experiments, assuming that there were small voids already present and that grew with the decreasing pressure. These voids could either be present because of a leak, or due to some volatiles boiling off from the resin at low pressure; assuming that the resin degassed during cure. In case of the A/900 experiments the voids were generated due to the lack of resin in the region closer to the inlet and vent positions. The assumption here was that due to the release of compaction, the fibre reinforcement absorbed resin from the region surrounding the inlet and vent positions. All of the A/C experiments, with each of the three materials, produced laminates with negligible void content, but having slight thickness gradients. The A/900 experiment produced negligible void content at the inlet, but significant void content at the vent because of the lack of resin locally during the post-filling stage.

Discussion and recommendations for industry

Process variations

Although clamping the inlet in the post-filling stage produced laminates with lower void content, the average fibre volume fraction of these laminates was lower than that achieved through the A/0 infusions. Moreover, when clamping the inlet, the operator does not have control over the final resin pressure and laminate thickness (or V_F). In fact, this is only controlled by the resin flow through the brake, which can vary with the dimension of the brake region and creases in the vacuum bag. The reason for higher voids in the A/0 experiments are assumed to be the boiling of the resin at low pressure, and the increased size of the bubbles due to the lower resin pressure. Higher volume fractions achieved through the A/0 infusions were due to the greater compaction stress on the laminates throughout the post-filling stage, and removal of excess resin from the laminate as compared to A/C, A/500 and A/900 experiments.

Decreasing the pressure differential in the filling stage decreased the void content in the final laminate but significantly increased the filling time. Owing to slower resin filling, fewer voids were trapped within fibre bundles during the filling process.[34] Moreover, the smaller change in compaction pressure from the

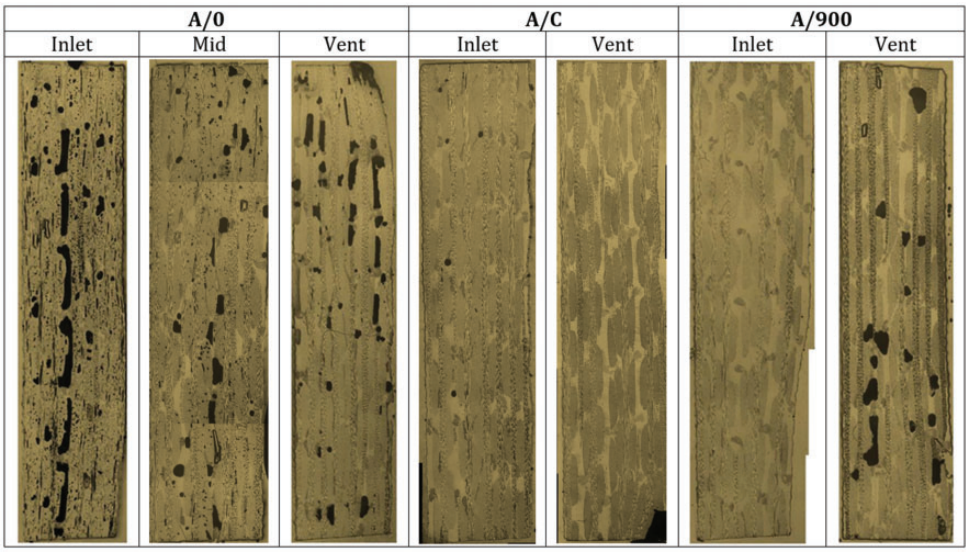

Figure 13. Cross-sectional microscopic images of EB-825 near inlet and vent.

filling to the post-filling stage reduced the void content. Another way the resin filling could be slowed down is due to dense and complicated fibre architecture. Hence, void content will be lower for reinforcements with tows in multiple directions[35] and the resin will impregnate the reinforcement completely.

A brake between the vent and the reinforcement was employed in all experiments. When the resin entered this brake region, it encountered high flow resistance towards the vent, causing the resin pressure in the remainder of the reinforcement to increase. The brake allows for the fibre bundles in the reinforcement to be saturated with resin completely at a higher pressure. It also minimises the amount of resin wastage through the vent, and reduces thickness gradients and variation of compaction history after filling.

Oosterom et al.[36] suggested that there is a significant variation in the achieved fibre volume fractions between different methods of vacuum application. The time between the end of filling and the application of the post-filling conditions was very critical, especially when decreasing the compaction pressure during post-filling (particularly for the A/900 experiments). When the post-filling conditions were applied, the vent pressure was reduced by 900 mbar and the reinforcement was decompressed, requiring more resin to fill in the gaps created due to the reduction in vacuum. Hence, the resin surrounding the reinforcement filled as much created volume in the reinforcement as was possible. Since there was not enough resin in the brake between the vent and the reinforcement, air was sucked in the reinforcement near the vent. The inlet end of the reinforcement did not experience similar air intake, as the reinforcement was already subjected to a low compaction and there was enough resin in the inlet tube to fill any volume created locally in the reinforcement. To avoid this, the onset of post-filling can be at the time when the pressure at Position 6 and the inlet has a difference of less than 150 mbar.

Recommendations

It was found that slower resin filling produced better laminates. There were two reasons why the resin filled slower in some experiments. One is the decreased pressure gradient and the other is the lower reinforcement permeability of certain reinforcements, which slowed down resin filling.

Based on Terzaghi's principle, given that the external atmospheric pressure remains constant, the control of the post-filling resin pressure inside the cavity can regulate the compaction stress applied on the reinforcement and thus the fibre volume fraction. The results from compaction characterisation of the reinforcements help to conclude that the compaction response of reinforcements can be used to predict the fibre volume fraction of manufactured parts. In addition, control of fibre volume fraction can be achieved through careful application of specific post-filling pressures. Moreover, during the process, using lower pressure difference between the inlet and vent in the filling stage decreased the final thickness gradient in the laminates. There will always be a difference between the resin pressure inside the mould and the compaction pressure during the VARTM process especially in the filling stage. The V_{FC} values were derived from a wet stack of fiber reinforcement and the V_{FP} values from a manufactured and dried or cured laminate. So it was assumed that the thickness of the wet laminate was equal to the thickness of the cured laminate.

The studied variations in the resin infusion process are operator governed. Creating a leak proof mould is the key to manufacturing quality parts using this process. Furthermore, the resin used must be introduced into the mould after ensuring that it is degassed properly to introduce the minimum possible voids in the manufactured parts. The post-filling pressure should also be chosen in accordance to the resin manufacturer specifications to avoid boiling off during cure.

The final part quality is a trade-off between higher fibre volume fraction and increased void content. It has been shown that a full vacuum post-filling creates a significant quantity of voids. However, from the presented compaction characterisation of fibre reinforcements it can be seen that a small reduction in vacuum level will have a relatively small effect on the fibre volume fraction, while potentially minimising void content. The marine industry, which often requires parts with a lower fibre volume fraction, or greater thicknesses to increase flexural stiffness, can concentrate on ensuring higher values of resin pressure and reduced void content. Moreover, the presented experiments showed that the parts manufactured under higher resin pressures (lower compaction stress) contained very low void content. Therefore, a very good quality part could be produced if the laminates are placed under higher resin pressures in the post-filling stage for the marine industry. Conversely, the aircraft industry required parts with higher volume fractions or lower thickness values. The presented experiments clearly showed that if full vacuum is pulled from both the inlet and vent in the post-filling stage, although the manufactured parts have an elevated fibre volume fraction, they concede a higher void content. Hence, a trade-off between the fibre volume fraction and void content in the manufactured part is required.

Conclusion

Evaluation was completed of the wet and dry compaction characteristics of three glass fibre reinforcements.

Compaction data indicated how to control laminate thickness and hence the fibre volume fraction of parts manufactured via the resin infusion technique, by applying pressure variations in the filling and post-filling stages. During manufacture of glass fibre epoxy composites, the filling of resin was accomplished at full vacuum and 650 mbar vacuum (350 mbar compaction pressure). Post-filling was accomplished by clamping the inlet, and/or application of full vacuum (995 mbar compaction pressure), 500 mbar of vacuum or 900 mbar of vacuum (100 mbar compaction pressure) at the inlet/vents. The effect of filling and post-filling pressures on the void content and the achieved fibre volume fraction of the manufactured part were studied. Analysis of the void content and the fibre volume fraction of the manufactured parts were presented in a number of ways. Void content was also analysed microscopically to find the distribution of voids as a result of reinforcement architecture, filling conditions, post-filling conditions and the post-filling strategy. It was established that the time delay in the conversion of the filling stage to the post-filling stage can be increased to minimise voids generated, particularly near the vent. Fibre volume fraction curves predicted using the compaction characterisation of the fibre reinforcements were plotted with the physically measured achieved fibre volume fractions of the manufactured laminates. It was verified that the achieved fibre volume fraction of manufactured parts can be predicted through the compaction characterisation of fibre reinforcements. Clamping the inlet in the post-filling stage is being widely used in industry, but the application of vacuum at the inlet in the post-filling stage not only increases the speed of post-filling but also produces laminates with higher fibre volume fraction. However, microscopic analysis carried out in this project indicated that higher fibre volume fraction is sometimes achieved at the cost of higher void content. Hence, the selection of vent post-filling pressure is a trade-off between the fibre volume fraction and the void content.

Declaration of Conflicting Interests

The author(s) declared no potential conflicts of interest with respect to the research, authorship, and/or publication of this article.

Funding

The author(s) received no financial support for the research, authorship, and/or publication of this article.

References

1. Summerscales J and Searle TJ. Low-pressure (vacuum infusion) techniques for moulding large composite structures. *Proc IMechE, Part L: J Materials: Design and Applications* 2005; 219: 45–58.
2. Williams C, Summerscales J and Grove S. Resin infusion under flexible tooling (RIFT): A review. *Compos Part A: Appl Sci Manuf* 1996; 27: 517–524.
3. Dereims A, Troian R, Drapier S, et al. Simulation of liquid resin infusion process by finite element method. In: *15th European conference on composite materials,* Venice, Italy, 2012.
4. Dereims A, Drapier S, Bergheau J, et al. Industrial simulation of liquid resin infusion by the finite element method. In: *19th international conference on composite materials*, Montreal, Canada, 2013.
5. Govignon Q, Allen T, Bickerton S, et al. Monitoring variations in laminate properties through the complete resin infusion process. In: *Proceedings of SAMPE: From art to science: Advancing materials & process engineering conference*, Cincinnati, OH, USA, 2007.
6. Daval B and Bickerton S. Exploring the potential for laminate quality control using VARTM. In: *Proceedings of 36th international SAMPE technical conference*, San Diego, CA, 15–18 November 2004.
7. Acheson JA, Simacek P and Advani SG. The implications of fiber compaction and saturation on fully coupled VARTM simulation. *Compos Part A: Appl Sci Manuf* 2004; 35: 159–169.
8. Marquette P, Dereims A, Hugon M, et al. Simulation based solutions for industrial manufacture of large infusion composite parts. SAE Technical Paper, 2014.
9. Chen D, Arakawa K and Xu C. Reduction of void content of vacuum-assisted resin transfer molded composites by infusion pressure control. *Polym Compos* 2015; 36: 1629–1637.
10. Grimsley BW, Cano RJ, Hubert P, et al. Preform characterization in VARTM process model development. NASA Technical Reports Server, 2004.
11. Yenilmez B and Sozer EM. Compaction of e-glass fabric preforms in the vacuum infusion process: (a) use of characterization database in a model and (b) experiments. *J Compos Mater* 2013; 47: 1959–1975.
12. Yenilmez B, Senan M and Murat Sozer E. Variation of part thickness and compaction pressure in vacuum infusion process. *Compos Sci Technol* 2009; 69: 1710–1719.
13. Yenilmez B, Caglar B and Sozer EM. Pressure-controlled compaction characterization of fiber preforms suitable for viscoelastic modeling in the vacuum infusion process. *J Compos Mater* 2017; 51: 1209–1224.
14. Govignon Q, Bickerton S and Kelly PA. Simulation of the reinforcement compaction and resin flow during the complete resin infusion process. *Compos Part A: Appl Sci Manuf* 2010; 41: 45–57.
15. Tackitt KD and Walsh SM. Experimental study of thickness gradient formation in the vartm process. *Mater Manuf Process* 2005; 20: 607–627.
16. Grimsley BW, Hubert P, Song X-L, et al. Flow and compaction during the vacuum assisted resin transfer molding

process. In: *33rd international SAMPE technical conference - Advancing affordable materials technology*, Seattle, WA, USA, 5–8 November 2001, pp. 140–153.
17. Li J, Zhang C, Liang R, et al. Modeling and analysis of thickness gradient and variations in vacuum-assisted resin transfer molding process. *Polym Compos* 2008; 29: 473–482.
18. Kuentzer N, Simacek P, Advani SG, et al. Correlation of void distribution to VARTM manufacturing techniques. *Compos Part A: Appl Sci Manuf* 2007; 38: 802–813.
19. Daval B and Bickerton S. Exploring the potential for laminate quality control using VARTM. In: *Proceedings of 36th international SAMPE technical conference*, San Diego, CA, USA, 15–18 November 2004.
20. Caglar B, Yenilmez B and Sozer EM. Modeling of post-filling stage in vacuum infusion using compaction characterization. *J Compos Mater* 2015; 49: 1947–1960.
21. Eun SW. *Experimental study of the microvoids formation and transport in the vacuum assisted resin transfer molding process*. Master Thesis, Seoul National University, Korea, 2002.
22. Patel N, Rohatgi V and Lee LJ. Micro scale flow behavior and void formation mechanism during impregnation through a unidirectional stitched fiberglass mat. *Polym Eng Sci* 1995; 35: 837–851.
23. Rohatgi V, Patel N and Lee LJ. Experimental investigation of flow-induced microvoids during impregnation of unidirectional stitched fiberglass mat. *Polym Compos* 1996; 17: 161–170.
24. Patel N, Rohatgi V and Lee LJ. Influence of processing and material variables on resin-fiber interface in liquid composite molding. *Polym Compos* 1993; 14: 161–172.
25. Park CH, Bréard J, Saouab A, et al. Unified saturation and micro-macro voids method in Liquid Composite Molding. *Int J Mater Form* 2008; 1: 937–940.
26. Niggemann C, Young SS, Gillespie JW, et al. Experimental investigation of the controlled atmospheric pressure resin infusion (CAPRI) process. *J Compos Mater* 2008; 42: 1049–1061.
27. Timms M, Govignon Q and Bickerton S. Identifying sources of variability in the mechanical performance of resin infused textile composites. In: *The 9th international conference on textile composites (TexComp9)*, Newark, DE, USA, 2008.
28. Govignon Q, Bickerton S and Kelly P. Simulation of the complete resin infusion process. In: *The 9th international conference on flow processes in composite materials (FPCM-9)*, Montreal, QC, Canada, 2008.
29. Zhao L and Hu X. Autocatalytic curing kinetics of thermosetting polymers: A new model based on temperature dependent reaction orders. *Polymer* 2010; 51: 3814–3820.
30. Teyssandier F, Ivanković M and Love BJ. Modeling the effect of the curing conversion on the dynamic viscosity of epoxy resins cured by an anhydride curing agent. *J Appl Polym Sci* 2010; 115: 1671–1674.
31. Albertz J. Digital stereophotogrammetric system. *Int Arch Photogramm Rem Sens* 1984; 25: 1–7.
32. Govignon Q, Bickerton S, Morris J, et al. Full field monitoring of the resin flow and laminate properties during the resin infusion process. *Compos Part A: Appl Sci Manuf* 2008; 39: 1412–1426.
33. Modulus SH. *PRIME^{TM} 20LV epoxy infusion system*. 2010.
34. Trochu F, Ruiz E, Achim V, et al. Advanced numerical simulation of liquid composite molding for process analysis and optimization. *Compos Part A: Appl Sci Manuf* 2006; 37: 890–902.
35. Park CH, Lebel A, Saouab A, et al. Modeling and simulation of voids and saturation in liquid composite molding processes. *Compos Part A: Appl Sci Manuf* 2011; 42: 658–668.
36. Van Oosterom S, Allen T, Battley MA, et al. Evaluation of a variety of vacuum assisted resin infusion processes. In: *21st international conference on composite materials (ICCM-21)*, Xi'an, China, 20–25 August, 2017.